Using Majorana spin-1/2 representation for the spin-boson model

Pablo Schad and Alexander Shnirman
Institut für Theorie der Kondensierten Materie, Karlsruhe Institute of Technology, 76128 Karlsruhe, Germany

Yuriy Makhlin
L.D. Landau Institute for Theoretical Physics, acad. Semyonov av., 1a, 142432, Chernogolovka, Russia and Moscow Institute of Physics and Technology, 141700, Dolgoprudny, Russia

arXiv:1510.05838v2 [cond-mat.mes-hall] 7 Mar 2016

In this paper we resolve a contradiction between the fact that the method based on the Majorana representation of spin-1/2 is exact and its failure to reproduce the perturbative Bloch-Redfield relaxation rates. Namely, for the spin-boson model, direct application of this method in the leading order allows for a straightforward computation of the transverse-spin correlations, however, for the longitudinal-spin correlations it apparently fails in the long-time limit. Here we indicate the reason for this failure. Moreover, we suggest how to apply this method to allow, nevertheless, for simple and accurate computations of spin correlations. Specifically, we demonstrate that accurate results are obtained by avoiding the use of the longitudinal Majorana fermion, and that correlations of the remaining transverse Majorana fermions can be easily evaluated using an effective Gaussian action.

I. INTRODUCTION

Application of field-theoretical methods to spin systems is hampered by the non-Abelian nature of the spin operators[1]. To circumvent this problem, one can represent spin operators in terms of fermions or bosons and use standard field theory[2]. Several formulations have been suggested, including the Jordan-Wigner[3] and Holstein-Primakoff[4] transformations, the Martin[5] Majorana-fermion and Abrikosov[6] fermion representations as well as the Schwinger-boson[7–10] and slave-fermion[11–16] techniques.

Among other representations of spin operators the Majorana-fermion approach has a special property. In most other approaches the necessary extension of the Hilbert space requires taking into account additional constraints on the boson/fermion operators, which place the system to the physical subspace. As it was realized early on[17] and reemphasized recently[18], for the Majorana representation this complicating step is not needed. Moreover, it was further observed[19,20] that a wide class of spin correlation functions can be reduced to Majorana correlations of the same order, so that the spin correlation functions can be computed very efficiently. This, in particular, includes single-spin problems, like the Kondo problem or the spin-boson problem. In this case one avoids potentially complex vertex corrections to the external vertices, and spin-spin correlation functions are essentially given by single-particle fermionic lines rather than by loop diagrams.

Despite these advantages, the Majorana spin-1/2 representation is not used very often. One possible reason is that its application requires careful calculations. In particular, for the spin-boson model, application of this method allows for a straightforward computation of the correlation functions of the transverse spin components[20], using the lowest-order self-energy. However, for longitudinal-spin correlations, it fails in the long-time limit. Here we indicate the reason for this behavior. Moreover, we suggest an approach that allows one to use the Majorana-fermion representation as a convenient and accurate tool for generic spin correlations. More specifically, we demonstrate that accurate results are obtained in low orders by avoiding the use of the longitudinal Majorana fermion operator. Furthermore, we demonstrate that correlations of the remaining, transverse Majorana fermions can be easily evaluated using an effective Gaussian action.

Here we show, how this problem arises and how it can be solved. First, we do so, using the standard diagrammatic methods. Then we reformulate the problem, using the path-integral formalism. This path-integral analysis allows us also to formulate a generalized Wick theorem and to provide a prescription for efficient computation of spin correlation functions. Finally, we demonstrate that the method indeed produces the expected longitudinal-spin correlations.

II. SPIN-BOSON MODEL

The spin-boson model[21] describes a spin-1/2 in a finite magnetic field. One of the transverse components of the spin is coupled to the bosonic bath. The Hamiltonian reads

$$H = B\hat{S}^z + \hat{X}\hat{S}^x + H_B\,, \tag{1}$$

where H_B is the Hamiltonian of the bosonic bath, which governs the free dynamics of $\hat{X}$. The bath is characterized by the correlation function $\Pi(\tau-\tau') \equiv \langle TX(\tau)X(\tau')\rangle$. In the Matsubara representation the correlation function

$\Pi(\tau-\tau')$ can be written as

$$\Pi(i\omega_m)=\int\limits_{-\Lambda}^{\Lambda}\frac{dx}{\pi}\,\frac{\rho(|x|)\,\mathrm{sign}\,x}{x-i\omega_m}\ , \tag{2}$$

where $\rho(|x|)$ is the bath spectral density, and $\omega_m=2\pi mT$. In the Ohmic case considered here $\rho(|x|)=g|x|$. For $\omega_m\ll\Lambda$ this gives $\Pi(i\omega_m)\approx(2g/\pi)\Lambda-g|\omega_m|$.

In the weak coupling limit, $g\ll 1$, the spin-boson model can be solved very efficiently by the master equation (Bloch-Redfield) technique[22,23]. In this limit the dynamics is characterized by two rates, Γ_1 and $\Gamma_2=\Gamma_1/2$. The dephasing rate Γ_2 describes the relaxation of the transverse spin components $\hat{S}_x$ and $\hat{S}_y$ to their equilibrium values, $\langle S_x\rangle=\langle S_y\rangle=0$. The rate Γ_1 describes the relaxation of the longitudinal component $\hat{S}_z$ to its equilibrium value $\langle S_z\rangle=(1/2)\tanh[\beta B/2]$. One readily obtains

$$\Gamma_1=2\Gamma_2=\frac{gB}{2}\coth[\beta B/2]\ . \tag{3}$$

From this one immediately concludes that the symmetrized, real-time correlation functions of the transverse spin components, $2\langle\{S_x(t_1),S_x(t_2)\}_+\rangle$ and $2\langle\{S_y(t_1),S_y(t_2)\}_+\rangle$, are given in the frequency domain by Lorentzians of unit weight and width Γ_2. In contrast, the longitudinal correlation function $2\langle\{S_z(t_1),S_z(t_2)\}_+\rangle$ consists in the Fourier representation of a delta function (zero-width Lorentzian) of weight $4\langle S_z\rangle^2$ and a Lorentzian of width Γ_1 and weight $1-4\langle S_z\rangle^2$. In Ref. 20 an attempt was made to employ the Majorana representation described in Appendix A and, specifically, the reduction (A4) to reproduce these well established facts. For the transverse correlation functions these results were indeed reproduced, and the calculation was significantly simpler than any of those attempting to calculate the fermionic loop. Yet, for the longitudinal correlations a result was obtained, which failed in the long-time limit. Namely, instead of two Lorentzians (one with zero width and the other with width Γ_1) a single Lorentzian with the width $\tilde{\Gamma}_1=\Gamma_1\left(1-\tanh^2[\beta B/2]\right)$ and unit weight was found. This solution reproduces correctly the short-time ($|t_1-t_2|\ll 1/\Gamma_1$) decay of the longitudinal correlation function, but fails in the long-time limit. Indeed, the wrong solution decays to zero, whereas the correct one should decay to $4\langle S_z\rangle^2$.

The reason for the failure is intuitively clear. In Eq. (A3) the spin operator $\hat{S}_z$ is essentially represented by the Majorana operator $\hat{\eta}_z$. The latter, however, is zero on average. Yet, since the Majorana representation is definitely valid, a resolution of the problem is needed.

III. DIAGRAMMATIC ANALYSIS

In this section we show that from the technical viewpoint the discussed failure of the diagrammatic calculation at long times arises from the insufficiency of the lowest-order approximation for the self-energy. In Section V we propose a method to circumvent this problem.

In the Majorana representation (A1) the Hamiltonian of the system reads

$$H=B\hat{S}^z+\hat{S}^x\,\hat{X}+H_B=-iB\,\hat{\eta}_x\hat{\eta}_y-i\hat{\eta}_y\hat{\eta}_z\,\hat{X}+H_B\ . \tag{4}$$

We employ the standard diagrammatic rules for calculations perturbative in the spin-bath interaction. The zeroth-order Green function of the Majorana fermions is obtained from

$$[G^0]^{-1}=\begin{pmatrix}-\delta(\tau-\tau')\partial_{\tau'} & iB\delta(\tau-\tau') & 0\\ -iB\delta(\tau-\tau') & -\delta(\tau-\tau')\partial_{\tau'} & 0\\ 0 & 0 & -\delta(\tau-\tau')\partial_{\tau'}\end{pmatrix}\ . \tag{5}$$

The Green function is given by the Dyson equation $[G]^{-1}=[G^0]^{-1}-\hat{\Sigma}$, where the matrix of the self-energies $\hat{\Sigma}$ has only two diagonal components, $\Sigma_{yy}\equiv\Sigma_y$ and $\Sigma_{zz}\equiv\Sigma_z$.

A. First order

We start by calculating the self-energies in the first order in g. Diagrammatically this corresponds to Fig. 1. We

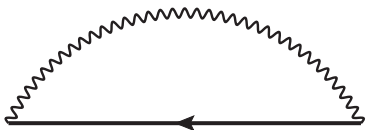

FIG. 1: The first-order diagram for the self-energy. It also corresponds to the saddle-point self-energy in the path-integral approach. Solid line: fermionic Green function, wavy line: bosonic (bath) correlator.

obtain

$$\Sigma_y^{(1)}(\tau-\tau') = \Pi(\tau-\tau')G_{zz}^0(\tau-\tau') \ , \tag{6}$$

$$\Sigma_z^{(1)}(\tau-\tau') = \Pi(\tau-\tau')G_{yy}^0(\tau-\tau') \ . \tag{7}$$

We use

$$G_{zz}^0(\epsilon_n) = \frac{1}{i\epsilon_n} \quad , \quad G_{yy}^0(\epsilon_n) = \frac{1}{2}\left[\frac{1}{i\epsilon_n - B} + \frac{1}{i\epsilon_n + B}\right] \ . \tag{8}$$

This gives

$$\Sigma_y^{(1)}(i\epsilon_n) = -\frac{1}{2}\int\limits_{-\Lambda}^{\Lambda}\frac{dx}{\pi}\,\frac{gx\coth[\beta x/2]}{x - i\epsilon_n} \ . \tag{9}$$

and

$$\Sigma_z^{(1)}(i\epsilon_n) = -\frac{1}{4}\sum_{\gamma=\pm 1}\int\limits_{-\Lambda}^{\Lambda}\frac{dx}{\pi}\,\frac{gx\left[\coth[\beta x/2] - \tanh[\beta\gamma B/2]\right]}{x - i\epsilon_n - \gamma B} \ . \tag{10}$$

Upon analytic continuation we obtain the retarded self-energies. For the transverse component we find

$$\mathrm{Im}\Sigma_y^{(1)}(i\epsilon_n \to \pm B + i0) = -\Gamma_1 \, , \tag{11}$$

where Γ_1 is the standard longitudinal relaxation rate given by Eq. (3). Note that upon substitution to the Dyson equation $[G]^{-1} = [G^0]^{-1} - \hat{\Sigma}$ this gives the following denominator for the transverse Green function: $G_\perp(\epsilon) \sim \left[\epsilon(\epsilon + i\Gamma_1) - B^2\right]^{-1}$. Thus the poles have the imaginary part $\approx -\Gamma_1/2 = -\Gamma_2$, corresponding to the standard dephasing rate.

For the longitudinal component we obtain

$$\mathrm{Im}\Sigma_z^{(1)}(i\epsilon_n \to 0 + i0) = -\tilde{\Gamma}_1 \ , \tag{12}$$

where

$$\tilde{\Gamma}_1 = \Gamma_1\left(1 - \tanh^2[\beta B/2]\right) \ . \tag{13}$$

Thus we reproduce the problem noticed in Ref. 20. Instead of the anticipated solution of the type

$$G_{zz,anticipated}^R(\epsilon) = \frac{A}{\epsilon + i0} + \frac{1-A}{\epsilon + i\Gamma_1} \ , \tag{14}$$

where $A \equiv (2\langle S_z\rangle)^2 = \tanh^2[\beta B/2]$, we obtain

$$G_{zz,obtained}^R(\epsilon) = \frac{1}{\epsilon + i(1-A)\Gamma_1} \ . \tag{15}$$

One can easily observe that these solutions coincide in the limit $\epsilon \gg \Gamma_1$. Thus our lowest-order evaluation of the self-energy catches correctly the short-time limit, whereas the long-time limit ($t \gg 1/\Gamma_1$) needs further analysis.

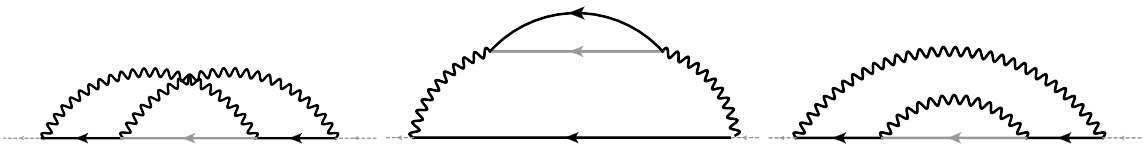

FIG. 2: Second-order diagrams for self-energy. The colors indicate the two flavors of Majorana fermions (y and z).

B. Second order

We first compare the self-energies corresponding to (14) and (15). For the anticipated solution we obtain

$$\Sigma_z^{anticipated}(\epsilon) = -i\,\frac{(1-A)\Gamma_1}{1+\frac{iA\Gamma_1}{\epsilon}} = -i(1-A)\Gamma_1 - \frac{A(1-A)\Gamma_1^2}{\epsilon + iA\Gamma_1}\,, \tag{16}$$

whereas in the lowest order we find $\Sigma_z^{(1)}(\epsilon) = -i(1-A)\Gamma_1$. We again observe the correspondence of the two for $|\epsilon| \gg \Gamma_1$. We expand (16) in powers of g and obtain

$$\Sigma_z^{anticipated}(\epsilon) = -i(1-A)\Gamma_1 - \frac{A(1-A)\Gamma_1^2}{\epsilon} + \dots\,. \tag{17}$$

Note that for $\epsilon < A\Gamma_1$ this series diverges and the expansion parameter in Eq. (17) is $A\Gamma_1/\epsilon$.

Eq. (17) suggests that the higher order in g terms in the expansion of the self-energy are singular. Thus we attempt to obtain (17) perturbatively in g. Below we calculate the next, second-order term of this expansion from the relevant second-order diagrams, which are shown in Fig. 2. For the first (leftmost in Fig. 2) diagram we obtain

$$\Sigma_z^{(2,1)}(\epsilon) = \frac{1}{\beta^2}\sum_{\omega_1,\omega_2} G_{yy}(\epsilon-\omega_1)G_{zz}(\epsilon-\omega_1-\omega_2)G_{yy}(\epsilon-\omega_2)\Pi(\omega_1)\Pi(\omega_2)\,. \tag{18}$$

The second (central in Fig. 2) diagram is given by

$$\Sigma_z^{(2,2)}(\epsilon) = \frac{1}{\beta^2}\sum_{\omega_1,\omega_2} G_{yy}(\epsilon-\omega_1)G_{zz}(\omega_1+\omega_2-\epsilon)G_{yy}(\epsilon-\omega_2)\Pi(\omega_1)\Pi(\omega_1)\,. \tag{19}$$

Both diagrams strongly diverge ($\propto \Lambda^2$), but their sum diverges at most logarithmically. Indeed it can be written as

$$\begin{aligned}\Sigma_z^{(2,12)}(\epsilon) &= \Sigma_z^{(2,1)}(\epsilon) + \Sigma_z^{(2,2)}(\epsilon)\\ &= -\frac{1}{2\beta^2}\sum_{\omega_1,\omega_2} G_{yy}(\epsilon-\omega_1)G_{zz}(\epsilon-\omega_1-\omega_2)G_{yy}(\epsilon-\omega_2)\left[\Pi(\omega_1)-\Pi(\omega_2)\right]^2\,.\end{aligned} \tag{20}$$

Evaluating this expression (with the help of Mathematica), we reproduced the second term of (17). All other diagrams, i.e., the third diagram (rightmost in Fig. 2) for Σ_z and all diagrams for Σ_y do not lead to $1/\epsilon$ divergences.

Thus we reproduce the anticipated expression for the longitudinal self-energy (16) up to the second order in g. This shows that the discrepancy noticed in Ref. 20 is removed by accounting for higher-order contributions to the self-energy of the longitudinal Majorana fermions. Thus we confirm the importance of higher-order corrections anticipated in Ref. 20 and also discussed in Ref. 24.

For a better understanding of this result, in the next section we develop a path-integral description (see also Refs. 25,26).

IV. PATH INTEGRAL FORMULATION

We use the Matsubara imaginary-time technique ($t = -i\tau$, $\partial_\tau = -i\partial_t$). The partition function, $Z = \int D[\dots]\exp[iS]$, reads

$$Z = \int D[X]D[\eta_\alpha]\,\exp\left\{ i\,S_B + \int_0^{1/T} d\tau\left[-\frac{1}{2}\,\eta_\alpha(\tau)\,\partial_\tau\eta_\alpha(\tau) + iB\eta_x\eta_y + i\eta_y\eta_z\,X\right]\right\}\,. \tag{21}$$

Here S_B is the free bosonic action. The first step is to average over the fluctuations of X, yielding

$$Z = \int D[\eta_\alpha] \exp\left\{ \int d\tau \left[-\frac{1}{2}\,\eta_\alpha(\tau)\,\partial_\tau\,\eta_\alpha(\tau) + i\,B\eta_x(\tau)\eta_y(\tau) \right] - \frac{1}{2}\int d\tau d\tau'\,\Pi(\tau-\tau')\,\eta_y(\tau)\eta_z(\tau)\,\eta_y(\tau')\eta_z(\tau') \right\} . \tag{22}$$

Next we decouple the quartic Majorana-Majorana interaction in a different channel. To this end we rearrange

$$\begin{aligned} iS_{int}[\eta_\alpha] &= -\frac{1}{2}\int d\tau d\tau'\,\Pi(\tau-\tau')\,\eta_y(\tau)\eta_z(\tau)\,\eta_y(\tau')\eta_z(\tau') \\ &= \frac{1}{2}\int d\tau d\tau'\,\Pi(\tau-\tau')\,\left[\eta_y(\tau)\eta_y(\tau')\right]\left[\eta_z(\tau)\eta_z(\tau')\right] . \end{aligned} \tag{23}$$

We now employ the Hubbard-Stratonovich transformation by introducing the fields Σ_y and Σ_z. These fields inherit the symmetry of the Majorana propagators, therefore $\Sigma_\alpha(\tau,\tau') = -\Sigma_\alpha(\tau',\tau)$. The new effective action reads

$$iS[\eta_\alpha,\Sigma_\alpha] = \frac{1}{2}\int d\tau d\tau'\,\eta_\alpha(\tau)\,\left(G^{-1}\right)_{\alpha,\beta}\,\eta_\beta(\tau') - \frac{1}{2}\int d\tau d\tau'\,\frac{\Sigma_y(\tau,\tau')\,\Sigma_z(\tau,\tau')}{\Pi(\tau-\tau')} . \tag{24}$$

The Majorana Green function in (24) is

$$G^{-1} = \begin{pmatrix} -\delta(\tau-\tau')\partial_{\tau'} & iB\delta(\tau-\tau') & 0 \\ -iB\delta(\tau-\tau') & -\delta(\tau-\tau')\partial_{\tau'} - \Sigma_y(\tau,\tau') & 0 \\ 0 & 0 & -\delta(\tau-\tau')\partial_{\tau'} - \Sigma_z(\tau,\tau') \end{pmatrix} . \tag{25}$$

The function $\Pi(\tau-\tau')$ is positive and non-zero. The standard form reads

$$\Pi(\tau-\tau') = \frac{g\pi T^2}{\sin^2(\pi T(\tau-\tau'))} . \tag{26}$$

The short-time divergence is to be cut off at $|\tau-\tau'| < 1/\Lambda$, leading to the maximal value of order $g\Lambda^2$.

The redecoupled action (24) is again quadratic in the Majorana Grassmann variables η_α, which allows us to integrate them out and to obtain an effective action of the Σ-fields:

$$iS[\Sigma_\alpha] = \frac{1}{2}\mathrm{Tr}\log\left(G^{-1}\right) - \frac{1}{2}\int d\tau d\tau'\,\frac{\Sigma_y(\tau,\tau')\,\Sigma_z(\tau,\tau')}{\Pi(\tau-\tau')} . \tag{27}$$

A. Saddle point

We can now identify the saddle point and fluctuations of the effective Σ-action. A saddle-point solution Σ_α^{sp} is found by expanding $\Sigma_\alpha = \Sigma_\alpha^{sp} + \delta\Sigma_\alpha$ ($\alpha = y, z$) around the saddle point and taking the linear order in $\delta\Sigma_\alpha$. We obtain

$$\Sigma_y^{sp}(\tau-\tau') = \Pi(\tau-\tau')G_{zz}^{sp}(\tau-\tau') , \tag{28}$$

$$\Sigma_z^{sp}(\tau-\tau') = \Pi(\tau-\tau')G_{yy}^{sp}(\tau-\tau') . \tag{29}$$

These equations look similar to Eqs. (6) and (7) obtained in the first order of the diagrammatic expansion (see Fig. 1). However, here in contrast to the first-order calculation, the fermionic lines should be broadened self-consistently. This means that the Green functions should be calculated using the Dyson equation $[G^{sp}]^{-1} = [G^0]^{-1} - \hat{\Sigma}^{sp}$.

Straightforward analysis shows that the self-consistency does not change the result considerably, and we again obtain the results given by Eqs. (9) and (10). However, we are still to investigate fluctuations around the saddle-point solution.

B. Role of the fluctuations

Reanalyzing the diagrams shown in Fig. 2 we understand that the third diagram is actually taken into account in the saddle-point calculation presented above. The first two diagrams of Fig. 2 correspond to fluctuations of the self-energy. This becomes evident if we redraw these diagrams as shown in Fig. 3. Thus these are the fluctuations around the saddle point which are responsible for the divergence of the longitudinal self-energy Σ_z. The first-order diagrammatic expansion corresponds to the saddle-point approximation and is insufficient for the longitudinal spin component.

FIG. 3: Second-order diagrams for the self-energy that correspond to fluctuations of the self-energy. The colors indicate the two flavors of Majorana fermions (y and z). These are the first two diagrams of Fig. 2.

V. GENERALIZED WICK THEOREM

The results obtained above allow us to formulate a prescription for efficient calculation of spin correlation functions of arbitrary order. This prescription essentially reduces to the suggestion to avoid η_z in all calculations. More specifically, in order to avoid divergences and the need to account for high-order contributions, one could use the following approach: for calculation of a spin correlation function replace S_x with η_x, S_y with η_y, and S_z with $\eta_x\eta_y$.

Indeed, consider the effective action with sources for the Majorana fermions:

$$\mathcal{S} = \frac{1}{2}\vec{\eta}^T([G^{sp}]^{-1} - \delta\Sigma)\vec{\eta} - \frac{1}{2}\frac{\delta\Sigma_z\delta\Sigma_y}{\Pi} + \vec{I}\vec{\eta}\,. \tag{30}$$

Here G^{sp} is the Green function at the saddle point, which can be obtained from (25) by replacing Σ by Σ^{sp}. In this expression and below in this section we use sloppy notations implying proper time integrations. Integrating over the Majorana fermions, we find

$$\mathcal{S} = \frac{1}{2}\,\mathrm{Tr\,Log}\left([G^{sp}]^{-1} - \delta\Sigma\right) - \frac{1}{2}\frac{\delta\Sigma_z\delta\Sigma_y}{\Pi} + \frac{1}{2}\vec{I}^T\left([G^{sp}]^{-1} - \delta\Sigma\right)^{-1}\vec{I}\,.$$

Since we are going to use only η_x and η_y, only the sources I_x and I_y will be relevant. In turn, this means that only the x, y components of $\left([G^{sp}]^{-1} - \delta\Sigma\right)$ will appear in the pre-exponential and will be averaged. These include only $\delta\Sigma_y$, but not $\delta\Sigma_z$.

Expansion of the Tr Log term to the second order gives

$$\delta\mathcal{S} = \frac{1}{2}\begin{pmatrix}\delta\Sigma_y & \delta\Sigma_z\end{pmatrix}\begin{pmatrix} G_y^{sp}G_y^{sp} & \Pi^{-1} \\ \Pi^{-1} & G_z^{sp}G_z^{sp}\end{pmatrix}\begin{pmatrix}\delta\Sigma_y \\ \delta\Sigma_z\end{pmatrix}$$

In Ref. 18 we have shown that the kernel $G_z^{sp}G_z^{sp}$ is small in the case $B = 0$. This observation applies here as well since B does not enter G_z^{sp}. This means that the $\langle\delta\Sigma_y\delta\Sigma_y\rangle$ correlator is small. Since only $\delta\Sigma_y$ is present in the pre-exponential, we do not have to take into account the fluctuations. This proves the Wick theorem for the saddle-point Green functions.

As an example, we employ the prescription to avoid η_z and the generalized Wick theorem introduced above to compute the longitudinal correlation function $2\langle\{S_z(t_1), S_z(t_2)\}_+\rangle$. Details of the calculation are given in Appendix C. The result reads

$$2\langle\{S_z(t_1), S_z(t_2)\}_+\rangle = 4\langle S_z\rangle^2 \cdot 2\pi\delta(\omega) + \left(1 - 4\langle S_z\rangle^2\right)\frac{2\Gamma_1}{\omega^2 + \Gamma_1^2}\,. \tag{31}$$

This is indeed the expected Bloch-Redfield result (cf. the discussion in Sec. II), which is consistent with Eq. (14).

VI. CONCLUSIONS

We conclude that the problem noticed first in Ref. 20 is apparently solved by taking into account fluctuations of the self-energy. In other words, calculations beyond the saddle-point approximation of Fig. 1 are needed. For the transverse components the saddle-point approximation is sufficient. Furthermore, efficient calculation is achieved if one uses only transverse Majorana operators.

VII. ACKNOWLEDGEMENTS

This research was funded by the German Science Foundation (DFG) through Grant No. SH 81/2-1 (PS and AS), by the German-Israeli Foundation (GIF) (AS), and by RSF under grant No. 14-12-00898 (dissipative dynamics; YM).

Appendix A: Majorana Representation for Spin-1/2 Operators

The following Majorana representation of the spin-1/2 operators was introduced by Martin[5] in 1959:

$$\hat{S}^{\alpha} = -\frac{i}{2}\epsilon_{\alpha\beta\gamma}\hat{\eta}_{\beta}\hat{\eta}_{\gamma}, \qquad \hat{S}^{x} = -i\hat{\eta}_{y}\hat{\eta}_{z}, \quad \hat{S}^{y} = -i\hat{\eta}_{z}\hat{\eta}_{x}, \quad \hat{S}^{z} = -i\hat{\eta}_{x}\hat{\eta}_{y}. \tag{A1}$$

The Majorana operators are Hermitian, $\hat{\eta}_{\alpha}^{\dagger} = \hat{\eta}_{\alpha}$, and obey the Clifford algebra $\{\hat{\eta}_{\alpha}, \hat{\eta}_{\beta}\} = \delta_{\alpha\beta}$, $\hat{\eta}_{\alpha}^{2} = 1/2$. It is easy to check that the representation (A1) perfectly reproduces the SU(2) algebra of the spin-1/2 operators $\hat{S}^{\alpha}$:

$$\left[\hat{S}^{\alpha}, \hat{S}^{\beta}\right] = i\epsilon_{\alpha\beta\gamma}\hat{S}^{\gamma} \quad , \quad \hat{\mathbf{S}}^{2} = 3/4 \; . \tag{A2}$$

The representation (A1) can be realized in various Hilbert spaces. The minimal Hilbert space is 4-dimensional and corresponds to two complex (Dirac) fermions, which we call $\hat{c}$ and $\hat{d}$. In this case one formally breaks the isotropy between the axes by choosing, e.g., $\hat{\eta}_{x} = (\hat{c} + \hat{c}^{\dagger})/\sqrt{2}$, $\hat{\eta}_{y} = (\hat{c} - \hat{c}^{\dagger})/\sqrt{2}i$, and $\hat{\eta}_{z} = (\hat{d} + \hat{d}^{\dagger})/\sqrt{2}$. Such a choice is termed "drone"-fermion representation and was used, e.g., in Ref. 17. Another, more symmetric option is to introduce an 8-dimensional Hilbert space corresponding to three complex fermions, $\hat{c}_{\alpha}$, where $\alpha = x, y, z$. In this case $\hat{\eta}_{\alpha} = (\hat{c}_{\alpha} + \hat{c}_{\alpha}^{\dagger})/\sqrt{2}$. As discussed in Ref. 18 the choice of the Hilbert space is irrelevant.

To obtain spin-spin correlation functions using (A1) one would have to calculate 4-fermion correlators or, more specifically, fermionic loops. In 2003 an observation was made[19,20], which allowed one to calculate just the (single-particle) Green functions of the Majorana fermions. Indeed, let us rewrite Eqs. (A1):

$$\hat{S}^{\alpha} = \hat{\Theta}\hat{\eta}_{\alpha}, \qquad \hat{\Theta} = -2i\hat{\eta}_{x}\hat{\eta}_{y}\hat{\eta}_{z}, \qquad \hat{\Theta}^{2} = 1/2. \tag{A3}$$

Apparently, the operator $\hat{\Theta}$ commutes with all three Majorana operators η_{α}. Hence, it also commutes with the spin operators, and thus with any physical Hamiltonian; thus the corresponding Heisenberg operator is time-independent. The average product of a pair of spin operators can now be represented as

$$\left\langle \hat{S}^{\alpha}(t_1)\hat{S}^{\beta}(t_2)\right\rangle = \left\langle \hat{\Theta}\hat{\eta}_{\alpha}(t_1)\hat{\Theta}\hat{\eta}_{\beta}(t_2)\right\rangle = \frac{1}{2}\left\langle \hat{\eta}_{\alpha}(t_1)\hat{\eta}_{\beta}(t_2)\right\rangle . \tag{A4}$$

Thus the average of two spin operators is expressed in terms of the average of only *two* Majorana fermions instead of four. Implications of this relation for time-ordered correlation functions in the Matsubara or Keldysh formalism are discussed in detail in Ref. 18.

Appendix B: Fluctuations in the Keldysh technique

For the Majorana Green function, the corresponding self-energy, and the bath correlator we use the following Keldysh structure,

$$\hat{G}_{\alpha}(\epsilon) = \begin{pmatrix} G_{\alpha}^{K}(\epsilon) & G_{\alpha}^{R}(\epsilon) \\ G_{\alpha}^{A}(\epsilon) & 0 \end{pmatrix}, \quad \hat{\Sigma}_{\alpha}(\epsilon) = \begin{pmatrix} 0 & \Sigma_{\alpha}^{A}(\epsilon) \\ \Sigma_{\alpha}^{R}(\epsilon) & \Sigma_{\alpha}^{K}(\epsilon) \end{pmatrix}, \quad \hat{\Pi}(\omega) = \begin{pmatrix} \Pi^{K}(\omega) & \Pi^{R}(\omega) \\ \Pi^{A}(\omega) & 0 \end{pmatrix} . \tag{B1}$$

The free Majorana Green functions are

$$G_{yy}^{0,R}(\epsilon) = \frac{1}{2}\left[\frac{1}{\epsilon - B + i0} + \frac{1}{\epsilon + B + i0}\right], \quad G_{zz}^{0,R}(\epsilon) = \frac{1}{\epsilon + i0}, \quad G_{\alpha\alpha}^{K}(\epsilon) = \tanh\left(\frac{\beta\epsilon}{2}\right)\left[G_{\alpha\alpha}^{R}(\epsilon) - G_{\alpha\alpha}^{A}(\epsilon)\right], \tag{B2}$$

and the spectral representation of the bath correlator $\hat{\Pi}^{ab}(t,t') = \left\langle \mathcal{T}_{K}\check{X}^{a}(t)\check{X}^{b}(t')\right\rangle$ in the Keldysh technique is given by

$$\Pi^{R/A}(\omega) = \int_{-\Lambda}^{\Lambda}\frac{dx}{i\pi}\frac{gx}{\omega + x \pm i0}, \qquad \Pi^{K}(\omega) = \coth\left(\frac{\omega}{2T}\right)\left(\Pi^{R}(\omega) - \Pi^{A}(\omega)\right) . \tag{B3}$$

In order to write the action in a Keldysh form, we introduce the vectors $\check{X}^{T} = (X^{cl}, X^{q})$ and $\check{\eta}_{\alpha}^{T} = (\eta_{\alpha}^{cl}, \eta_{\alpha}^{q})$ (we use the convention $X^{cl} = (X^{u} + X^{d})/\sqrt{2}$ and $X^{q} = (X^{u} - X^{d})/\sqrt{2}$) and the matrices $\gamma^{cl} = \mathbb{1}$, $\gamma^{q} = \tau_{1} \equiv \tau_{x}$ in the

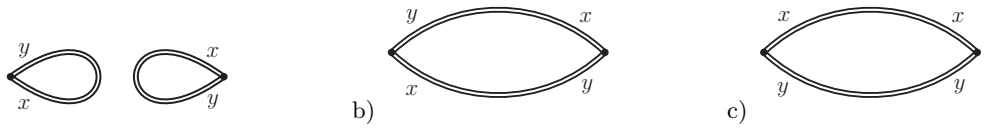

FIG. 4: Three contributions to the longitudinal spin correlation function. Double lines: fermionic saddle-point Green functions.

Keldysh space:

$$iS_{int} = -\int_C dt\, X(t)\eta_y(t)\eta_z(t) = -\frac{1}{\sqrt{2}}\int_{-\infty}^{\infty} dt\ \left(X^{cl}(t)[\check{\eta}_y^T(t)\gamma^q\check{\eta}_z(t)] + X^q(t)[\check{\eta}_y^T(t)\gamma^{cl}\check{\eta}_z(t)]\right) \tag{B4}$$

$$= -\frac{1}{\sqrt{2}}\sum_{a=q,cl}\int_{-\infty}^{\infty} dt\,(\tau_1\check{X}(t))^a[\check{\eta}_y^T(t)\gamma^a\check{\eta}_z(t)]\,. \tag{B5}$$

The contribution of the first diagram of Fig. 3 to the retarded self-energy $\Sigma^R = \Sigma^{q,cl}$ reads

$$\frac{1}{4}\sum_{a,b,c,d=q,cl}\int_{-\infty}^{\infty}\frac{d\omega_1 d\omega_2}{(2\pi)^2}\left(\gamma^a\hat{G}_y(\omega_2)\gamma^b\hat{G}_z(\omega_1+\omega_2)\gamma^c\hat{G}_y(\omega_1+\epsilon)\gamma^d\right)^{q,cl}\left(\tau_1\hat{\Pi}(\omega_2-\epsilon)\tau_1\right)^{ca}\left(\tau_1\hat{\Pi}(\omega_1)\tau_1\right)^{db}, \tag{B6}$$

while the second diagram contributes

$$-\frac{1}{4}\sum_{a,b,c,d=q,cl}\int_{-\infty}^{\infty}\frac{d\omega_1 d\omega_2}{(2\pi)^2}\,\mathrm{Tr}\{\hat{G}_y(\omega_2)\gamma^b\hat{G}_z(\omega_1+\omega_2)\gamma^c\}\left(\gamma^a\hat{G}_y(\omega_1+\epsilon)\gamma^d\right)^{q,cl}\left(\tau_1\hat{\Pi}(\omega_1)\tau_1\right)^{ca}\left(\tau_1\hat{\Pi}(\omega_1)\tau_1\right)^{db}. \tag{B7}$$

Both diagrams were evaluated using the spectral representation (B3). We found (with the help of Mathematica) that the result agrees with that obtained in the Matsubara technique and therefore confirms that the two diagrams in Fig. 3 are responsible for the divergent term in the expansion (17).

Appendix C: Longitudinal spin correlations

In this appendix we demonstrate how the generalized Wick theorem can be utilized in practice. To this end, we compute the longitudinal spin-spin correlation function $C_{zz}^{(2)}(t,t') = 2\left\langle\mathcal{T}_K S_z^{cl}(t)S_z^{cl}(t')\right\rangle$ employing the Keldysh technique. We avoid the longitudinal Majorana fermion η_z and use instead the relation $S_z = -i\eta_x\eta_y$. The correlator is, thus, given by

$$C_{zz}^{(2)}(t,t') = -\left\langle\mathcal{T}_K[\check{\eta}_x(t)\gamma^{cl}\check{\eta}_y(t)][\check{\eta}_x(t')\gamma^{cl}\check{\eta}_y(t')]\right\rangle\,. \tag{C1}$$

The generalized Wick theorem for saddle-point Green functions means that vertex corrections to the z-spin vertices are absent. Thus computing (C1) we obtain three contributions, which correspond to the diagrams in Fig. 4:

$$C_{zz}^{(2)}(\omega) \;=\; 2\pi\delta(\omega)\left(\int\frac{d\Omega}{2\pi}\,G_{xy}^{sp,K}(\Omega)\right)^2 - \int\frac{d\Omega}{2\pi}\,\mathrm{Tr}\left[\hat{G}_{xy}^{sp}(\Omega)\hat{G}_{xy}^{sp}(\Omega-\omega)\right] + \int\frac{d\Omega}{2\pi}\,\mathrm{Tr}\left[\hat{G}_{xx}^{sp}(\Omega)\hat{G}_{yy}^{sp}(\Omega-\omega)\right]. \tag{C2}$$

Here the traces are taken over the Keldysh indices. In order to perform the calculation we need the saddle-point Green functions of Majorana fields η_x and η_y. It is sufficient to calculate the retarded components of these Green functions, and we obtain

$$G_{xx}^{sp,R}(\epsilon) = \frac{\epsilon-\Sigma_y^{sp,R}(\epsilon)}{\epsilon\left(\epsilon-\Sigma_y^{sp,R}(\epsilon)\right)-B^2}\,,\qquad G_{yy}^{sp,R}(\epsilon) = \frac{\epsilon}{\epsilon\left(\epsilon-\Sigma_y^{sp,R}(\epsilon)\right)-B^2}\,,$$

$$G_{xy}^{sp,R}(\epsilon) = \frac{-iB}{\epsilon\left(\epsilon-\Sigma_y^{sp,R}(\epsilon)\right)-B^2}\,,\qquad G_{yx}^{sp,R}(\epsilon) = -G_{xy}^{sp,R}(\epsilon)\,. \tag{C3}$$

Here the retarded self-energy $\Sigma_y^{sp,R}(\epsilon)$ is (approximately) given by the analytic continuation of (9). It is sufficient to replace $\Sigma_y^{sp,R}(\epsilon)$ by its value in the vicinity of the poles $\epsilon\approx\pm B$, i.e., $\Sigma_y^{sp,R}(\epsilon)\to-i\Gamma_1$ (cf. (11)).

We can now calculate the longitudinal spin correlator $C^{(2)}_{zz}(\omega)$. We consider the limit of high magnetic field $B \gg \Gamma_1$. The first term in (C2), corresponding to Fig. 4a, yields a factor of $A = \tanh^2 \frac{B}{2T} = 4\langle S_z \rangle^2$. The second and third terms in (C2), i.e., Fig. 4b,c, both give rise to a Lorentzian of width Γ_1. Thus we obtain

$$C^{(2)}_{zz}(\omega) = A \cdot 2\pi\delta(\omega) + \frac{(1-A)\,2\Gamma_1}{\omega^2 + \Gamma_1^2} \ , \tag{C4}$$

which indeed coincides with the Bloch-Redfield result discussed in Sec. II.

---

[1] A. Altland and B. Simons, *Condensed Matter Field Theory* (Cambridge University Press, 2010), 2nd ed.
[2] A. M. Tsvelik, *Quantum field theory in condensed matter physics* (Cambridge University Press, Cambridge, 1996).
[3] P. Jordan and E. Wigner, Zeitschrift für Physik **47**, 631 (1928).
[4] T. Holstein and H. Primakoff, Phys. Rev. **58**, 1098 (1940).
[5] J. L. Martin, Proc. R. Soc. London A **251**, 536 (1959).
[6] A. A. Abrikosov, Physics **2**, 5 (1965).
[7] J. Schwinger, in *Quantum Theory of Angular Momentum*, edited by L. Biederharn and H. van Dam (Academic Press, New York, 1965), p. 229.
[8] D. P. Arovas and A. Auerbach, Phys. Rev. B **38**, 316 (1988).
[9] N. Read and S. Sachdev, Phys. Rev. Lett. **66**, 1773 (1991).
[10] F. Wang, Phys. Rev. B **82**, 024419 (2010).
[11] I. Affleck, Z. Zou, T. Hsu, and P. W. Anderson, Phys. Rev. B **38**, 745 (1988).
[12] J. B. Marston and I. Affleck, Phys. Rev. B **39**, 11538 (1989).
[13] N. Andrei and P. Coleman, Phys. Rev. Lett. **62**, 595 (1989).
[14] E. Dagotto, E. Fradkin, and A. Moreo, Phys. Rev. B **38**, 2926 (1988).
[15] X. G. Wen, Phys. Rev. B **44**, 2664 (1991).
[16] F. J. Burnell and C. Nayak, Phys. Rev. B **84**, 125125 (2011).
[17] H. J. Spencer, Phys. Rev. **171**, 515 (1968).
[18] P. Schad, Y. Makhlin, B. Narozhny, G. Schön, and A. Shnirman, Annals of Physics **361**, 401 (2015).
[19] W. Mao, P. Coleman, C. Hooley, and D. Langreth, Phys. Rev. Lett. **91**, 207203 (2003).
[20] A. Shnirman and Y. Makhlin, Phys. Rev. Lett. **91**, 207204 (2003).
[21] A. J. Leggett, S. Chakravarty, A. T. Dorsey, M. P. A. Fisher, A. Garg, and W. Zwerger, Rev. Mod. Phys. **59**, 1 (1987).
[22] F. Bloch, Phys. Rev. **105**, 1206 (1957).
[23] A. Redfield, IBM Journal of Research and Development **1**, 19 (1957).
[24] S. Florens, A. Freyn, D. Venturelli, and R. Narayanan, Phys. Rev. B **84**, 155110 (2011).
[25] V. R. Vieira, Phys. Rev. B **23**, 6043 (1981).
[26] V. R. Vieira, Physica A: Statistical Mechanics and its Applications **115**, 58 (1982).